Anomalous Dynamics of Hydration Water in Carbohydrate Solutions

Matías H. H. Pomata

Departamento de Física, Comisión Nacional de Energía Atómica-CNEA, Avenida Gral. Paz 1499 (1650) San Martín, Buenos Aires, Argentina

Milton T. Sonoda

Universidade Federal de Uberlandia, Avenida Jose Joao Dib, 2545 Ituiutaba, MG, 38302-000 Brazil

Munir S. Skaf*

Institute of Chemistry, State University of Campinas—UNICAMP, P. O. Box 6154, Campinas, SP, 13084-862 Brazil

M. Dolores Elola*

Departamento de Física, Comisión Nacional de Energía Atómica—CNEA, Avenida Libertador 8250, (1429) Buenos Aires, Argentina

Received: April 30, 2009; Revised Manuscript Received: July 8, 2009

Molecular dynamics simulations have been carried out to investigate the dynamics of fructose aqueous solutions up to 70 wt % concentration. We find that the hydrogen (H)-bonded network of fructose molecules extends with increasing sugar content and forms a structurally heterogeneous system around and above 45 wt % concentration, characterized as a percolated-like solute domain permeated by patchy regions of solvent. The presence of such aggregates in concentrated solutions promotes the slowing down of water translational, reorientational, and H-bonding dynamics, typical of many biomolecular environments. Analysis of the effects of the topological and energetic disorder of the sugar aggregates on vicinal water dynamics, similar to that recently carried out for the hydration layer of proteins by Pizzitutti et al. *(J. Phys. Chem. B* **2007**, *111*, 7584), reveals many similarities between the dynamical anomaly of the hydration layers of both systems. Like a protein surface, topological and energetic disorders of the sugar aggregates both contribute to the translational diffusion anomaly. However, unlike in the vicinity of a protein surface, the rotational relaxation is also hindered by the topological disorder created by the intertwined, percolating sugar clusters in concentrated solutions.

I. Introduction

The study of the properties of saccharides in aqueous mixtures is relevant to many areas of basic sciences, such as chemistry, biology, and medicine, and presents multiple applications in the food and pharmacological industries.[1,2] One of the most striking characteristics of carbohydrate solutions is the marked rise in the viscosity as the sugar content increases.[3] At a molecular level, these changes are the manifestation of important structural and dynamical modifications, most notably those associated with the formation of sugar aggregates[4] and an extraordinary slowing down of water mobility.[5] From a practical point of view, both phenomena represent key features in determining the action of carbohydrate solutions as food preservers and inhibitors of chemical degradation in pharmaceutical products.

The structural and dynamical modifications are very much correlated. The overall dynamical features of saccharide solutions arise from the complex interplay between water−sugar and sugar−sugar interactions, which are basically established through hydrogen bond interactions. As a result, whereas the mobility of water decreases linearly with sugar content at low concentrations, the deviations from linearity at high concentrations have been attributed to the formation of sugar clusters. The presence of these sugar aggregates hinders the mobility of water molecules to such an extent that the diffusive translational and reorientational characteristic times may be lengthened up to 1 order of magnitude compared to those observed in bulk water. Experimental evidence of this effect arises from results obtained from different techniques, including NMR,[3−6] dielectric relaxation,[7,8] and neutron scattering.[9,10] Computer simulations of carbohydrate−water systems have also corroborated this picture.[11−15] A simplified interpretation of the complex dynamics occurring in the real systems is that in which water molecules can be essentially assigned to two states: bound to saccharides or "free" (i.e., as in the neat liquid). Sugar-bound water molecules are expected to exhibit a much slower dynamics than free water. As a result, water dynamics in carbohydrate solutions would resemble in many ways that of other biomolecular confining environments such as in the interior of reversed micelles,[16,17] around DNA strands,[18−20] and surrounding protein surfaces.[21−25]

The nature of water dynamics around a protein has been recently investigated by Pizzitutti et al.[25] by means of molecular dynamics simulations. The simulations show that the dynamic hindrance of water surrounding the protein is accompanied by an anomalous behavior of the hydration layer, characterized by a sublinear time dependency of the translational diffusive motions and a highly nonexponential rotational relaxation,

* To whom correspondence should be addressed. E-mail: skaf@iqm.unicamp.br (M.S.S.); DoloresElola@gmail.com (M.D.E.).

10.1021/jp904019c CCC: $40.75
Published on Web 09/09/2009

typical of glassy states. Their analyses have provided insights into the separate roles played by the protein motion, spatial surface roughness (topological disorder), and the energetic landscape created by H-bonding pinning sites (energetic disorder) on the anomalous dynamics of the hydration layer. The authors have found that both topological and energetic disorders underlie the anomalous translational diffusion, whereas rotational relaxation seems insensitive to the protein topological disorder and is influenced by the electrostatic energetic landscape alone. Protein motion, in turn, diminishes the anomalous behavior.

As for saccharide solutions, it is not fully understood how the sugar molecules and their increasing molecular aggregation with concentration impair the mobility of the solvent. In particular, it is not known whether the dynamics of the hydration layer exhibits an anomalous behavior similar to that found around a protein surface. Are the molecular mechanisms underlying water dynamical hindrance in protein and carbohydrate solutions of the same nature? Are translational and rotational dynamics affected by both types of disorder in saccharide solutions? Largely motivated by the work of Pizzitutti et al.[25] and our own recent study on the structure and dynamics in carbohydrate aqueous solutions,[15] we have attempted to answer some of these questions by performing molecular dynamics (MD) simulations of fructose solutions up to 70 wt % concentration. In our previous work,[15] we observed the onset of what looks as a sharp "percolative" transition of solute aggregates at sugar concentrations close to 3.8 M, indicating a possible connection between this global structural modification and the observed lengthening of mostly all characteristic time scales describing solvent dynamics. In the present work, we aim at investigating the nature of the dynamics of the hydration layer for the most concentrated solution using the approach adopted for proteins[25] in which the sugar aggregates are pictured as a mesoscopic domain that fluctuates slowly in time in comparison to the rest of the system. We examine how sugar aggregate dynamics and its spatial roughness and H-bonding features affect the translational and reorientational motions of the hydration layer.

This paper is organized as follows: in section II we describe the systems studied and the potential models, along with simulation details. In section III we present and discuss the results obtained for the dynamical and structural properties. Finally, we conclude in section IV with a summary of our main findings.

II. Systems Studied and Simulation Details

The computer simulations results presented in this paper correspond to aqueous solutions of mixtures of two of the most abundant fructose tautomers, namely, β-D-fructopyranose and β-D-fructofuranose, with 70% and 30% relative abundance, respectively. Additional details are given in ref 15. We focused our attention on solutions with high sugar content, i.e., those with fructose concentrations intermediate between $c = 3$ and 5 M. As a reference, a few additional runs were performed on 1 M solutions and pure water systems as well. The number of molecules and simulation box dimensions of the simulated systems are shown in Table 1 and correspond to the experimental densities. The OPLS-AA force field was used to model interactions involving the carbohydrates.[26] Unlike our previous work, in which we used SPC water, we adopted here the classical SPC/E model[27] because it reproduces better the dynamics of water.

The MD trajectories were generated using the NAMD package[28] and corresponded to the microcanonical ensemble, at temperatures close to ambient conditions. Initial configurations were generated using the PackMol software.[29] Short-ranged intermolecular forces were cut off at half the simulation box length, and the particle mesh Ewald (PME) method was used for long-range Coulomb forces. The equations of motion were integrated using a multiple time step integration scheme, with a time step of 2 fs.

TABLE 1: Simulation Parameters: Fructose Concentration (c), Cubic Box Length, and Corresponding Number of Fructopyranose (N_{PYR}), Fructofuranose (N_{FUR}), and Water (N_w) Molecules

c (M)	c (wt %)	L (Å)	N_{PYR}	N_{FUR}	N_w
0	0	24.65	0	0	500
1	17	28.55	10	4	686
3	45	30.78	37	16	647
3.5	51	31.54	46	20	634
4	57	32.70	57	25	618
5	68	37.98	116	50	792

The initial equilibration procedure involved running preliminary trajectories for about 500 ps, at 450 K. Subsequent cooling runs of similar length were performed, until the systems were finally equilibrated at $T \sim 298$ K. After equilibration, trajectory analyses were performed along simulation runs lasting typically 20 ns.

In order to study in greater detail the dynamics of the most concentrated system (5 M), we performed additional runs, corresponding to two "surrogate" systems:[25,30] The first (Fruc-FR) was built by freezing the fructose molecules, but allowing the water molecules to move (properly thermalized at 298 K). Initial states for Fruc-FR runs were randomly chosen from configurations generated in previous, fully dynamical, trajectories (hereafter referred to as Fruc-FD). Comparison between Fruc-FD and Fruc-FR runs allows examining the effects of the saccharide motions on water dynamics. From the Fruc-FR system, the effects of the (now static) topological disorder can be singled out from those due to the energetic disorder by switching off the Coulombic interactions between the polar groups of the solute and water, thus generating the second system (Fruc-LJ).

III. Results

A. Translational and Orientational Dynamics. We will start our analysis by investigating changes in some relevant dynamical observables associated with the overall translational and rotational dynamics of solute and solvent molecules in fructose solutions of increasing sugar concentrations.

The molecular translational mobility of the different species can be conveniently described in terms of the time evolution of the mean-squared center of mass displacements

$$\mathscr{R}^2(t) = \langle |\mathbf{r}_i(t) - \mathbf{r}_i(0)|^2 \rangle \quad (1)$$

where the angular brackets denote a statistical average. The classical Einstein expression[31]

$$6Dt = \lim_{t \to \infty} \mathscr{R}^2(t) \quad (2)$$

has been used to obtain self-diffusion coefficients for water (D_w) and fructose molecules (D_F).

Results for D_w and D_F, are listed in Table 2 and plotted in the two panels of Figure 1, where we also display results from

TABLE 2: Self-Diffusion Coefficients D (in 10^{-5}cm^2/s) and Typical Translational Time τ_w (in ps) Obtained for the Systems Studied

c (M)	D_F	D_w	τ_w
0	–	2.4[a]	6.2
1	0.30[b]	1.8[a]	7.5
3	0.18[b]	0.73[a]	16.8
4	0.05[b]	0.44[b]	21.2
5	0.02[b]	0.17[b]	70.2

[a] A 100−2000 ps time window was used for the linear fit of $\mathcal{R}^2(t)$. [b] A 1000−2000 ps time window was used for the linear fit of $\mathcal{R}^2(t)$.

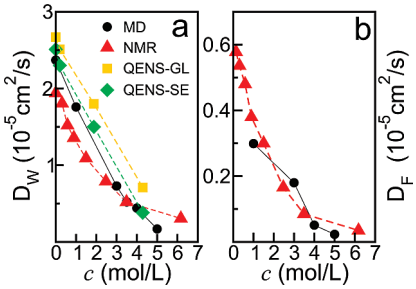

Figure 1. Self-diffusion coefficients obtained from MD simulations for (a) water and (b) fructose species, as a function of fructose concentration. Experimental data were taken from ref 5 (NMR) and ref 9 (QENS).

NMR[5] and quasielastic neutron scattering (QENS) experiments.[9] Interestingly, predictions from simulation experiments reproduce the sharp drops exhibited by the experimental diffusion coefficients quite accurately. The agreement between MD and experimental results in the present case is far superior than we previously reported using SPC water solutions.[15] A characteristic translational time for water can be inferred from τ_w, the time required by a water molecule to cover a distance equivalent to its own diameter, say ∼3 Å. Results for τ_w appear in the last column of Table 2. One can clearly observe a sharp increase as one surpasses $c \sim 4$ M, and an overall retardation of approximately 1 order of magnitude as one moves from pure water to 5 M fructose: on average, a water molecule travels a distance of 3 Å in 6 ps in the neat liquid, whereas it takes about 70 ps to cover the same distance in the 5 M solution.

The single-particle orientational dynamics of both species is described in terms of time correlation functions (TCF)

$$C_l^e(t) = \langle P_l[\mathbf{e}_i(0)\cdot\mathbf{e}_i(t)]\rangle \quad (3)$$

where $P_l(x)$ is the lth order Legendre polynomial and $\mathbf{e}_i$ is a representative unit vector fixed to the molecular frame. The first-rank orientational TCFs for the dipole moments, $C_1^\mu(t)$, for water and fructose species are displayed in Figure 2. In pure liquids, the long-time diffusive portions of these curves are normally well adjusted assuming either single or biexponential decays, whereas estimations of the overall characteristic orientational time, τ_μ, can be obtained from time integrals of the corresponding TCFs. In the present case, the reorientational relaxation is best described by a combination of biexponential and stretched exponential functions

$$C_l^e(t) \sim a_1 e^{-t/\tau_1} + a_2 e^{-t/\tau_2} + a_3 e^{-(t/\tau)^\beta} \quad (4)$$

The overall relaxation time τ_μ becomes

$$\tau_\mu = \int_0^\infty C_1^\mu(t)\,dt = a_1\tau_1 + a_2\tau_2 + \frac{a_3\tau}{\beta}\Gamma(1/\beta) \quad (5)$$

where Γ is the gamma function. Best fitting parameters for the first-rank dipolar correlation function, $C_1^\mu(t)$, are displayed in Table 3, along with the characteristic orientational times τ_μ. Modifications in the characteristic rotational time scales follow a similar trend to that observed for the diffusive modes. However, in this case, the variations in all τ_μ are much more prominent. At 5 M, the rotational dynamics of water is practically 2 orders of magnitude slower than in pure water. Slowing down of the rotational dynamics of the saccharides molecules is even more pronounced than for the solvent. Above 2 M, particularly, the characteristic time scales of sugar reorientation sharply surpass the nanosecond time regime.

B. Hydrogen Bonding and Clustering. In pure water, it is well established that hydrogen bond (HB) dynamics is dictated to a large extent by a combination of translational and reorientational motions.[32,33] In recent works, Laage and Hynes proposed a molecular mechanism of water reorientation based on the extended jump model. In their model, water reorientation occurs through large amplitude angular jumps due to exchange of HB acceptors, with only a minor contribution from diffusive modes.[34,35] Here, it is of interest to investigate how the presence of the sugar molecules influences the dynamics of formation and breaking of HBs. Following previous studies,[36,37] our analysis is based on the intermittent H-bond correlation function

$$C_{HB}(t) = \frac{\langle \eta_{ij}(0)\eta_{ij}(t)\rangle}{\langle \eta_{ij}^2\rangle} \quad (6)$$

where the characteristic function $\eta_{ij}(t) = 1$ if molecules i and j are H-bonded at time t and zero otherwise. We use a geometrical criterion to define H-bonding,[15,32,38] a pair of molecules is considered to be H-bonded if their relative position is such that (i) the O···H separation is smaller than 2.6 Å, (ii) the O···O distance is not larger than 3.5 Å, and (iii) the angle O···O−H is smaller than 30°.

Figure 3 shows $C_{HB}(t)$ obtained for the different sugar solutions and for pure water. The correlation functions corresponding to HBs between water molecules decay at a much faster rate than those associated with fructose−water pairs and even much faster when compared to fructose−fructose HBs. A fitting similar to that shown in eq 4 yields an excellent match

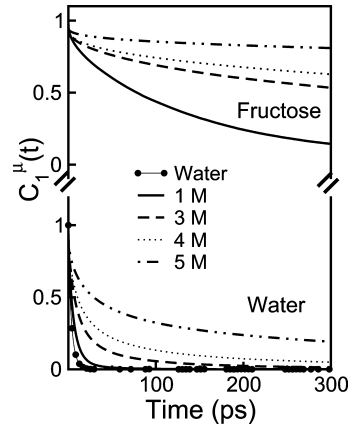

Figure 2. Single-molecule first-order dipole time correlation functions of water (bottom curves) and fructose species (upper curves) in solution.

TABLE 3: Stretched-Plus-Biexponential Fitting Parameters to $C_\mu(t)$ for Water and Fructose Species at Different Concentrations and Typical Reorientational Times Obtained from Eq 5[a]

	first-rank single dipole correlations							
c (M)	a	τ	β	a_1	τ_1	a_2	τ_2	τ_μ
				water				
0	0.0	–	–	0.15	0.30	0.85	5.9	5.0
1	0.42	3.5	0.47	0.58	6.6	0.0	–	7.0
3	0.52	13.2	0.42	0.35	9.5	0.11	32.9	27.4
3.5	0.54	21.9	0.42	0.28	9.6	0.14	29.9	42.6
4	0.68	25.2	0.39	0.21	11.2	0.11	40.3	68.4
5	0.81	112	0.37	0.10	16.3	0.07	63.3	384
				fructose[b]				
1	0.48	135	0.61	0.46	141	0.0	–	160
3	0.67	956	0.36	0.31	592	0.0	–	3110

[a] Times are given in picoseconds. [b] The decays for the rotational dynamics for fructose concentrations larger than 3 M are exceedingly slow to be adequately captured by the simulation experiment.

TABLE 4: Stretched-Plus-Biexponential Fitting Parameters to $C_{HB}(t)$ for W−W and F−W Pairs at Different Concentrations and H-Bond Typical Relaxation Times Obtained from Time Integrals of the Fitting Functions[a]

	H-bond correlation function							
c (M)	a_3	τ	β	a_1	τ_1	a_2	τ_2	τ_{HB}
				water−water				
0	0.28	0.74	0.34	0.46	2.3	0.27	3.9	3.3
1	0.31	1.5	0.35	0.46	3.8	0.23	7.6	5.8
3	0.44	4.2	0.35	0.38	5.8	0.19	16.8	14.4
3.5	0.47	5.2	0.35	0.34	6.5	0.19	19.3	18.0
4	0.53	6.6	0.35	0.30	6.8	0.17	22.6	23.7
5	0.67	18.7	0.34	0.19	10.7	0.14	39.4	77.4
				fructose−water				
1	0.44	3.5	0.37	0.32	8.4	0.24	25.4	15.2
3	0.64	16.3	0.39	0.23	22.1	0.12	98.2	54.1
3.5	0.68	24.2	0.38	0.19	23.6	0.12	99.9	79.8
4	0.73	30.9	0.37	0.17	28.5	0.10	125.1	111.1
5	0.73	103.1	0.29	0.11	40.8	0.15	240.2	858.3

[a] Times are given in picoseconds.

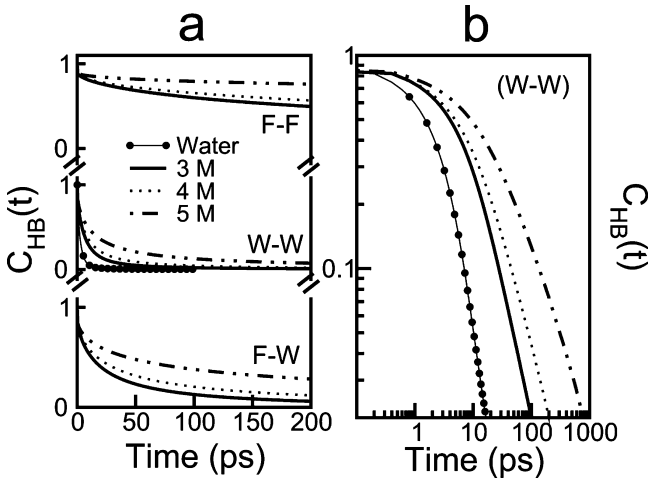

Figure 3. Intermittent H-bond correlation function, $C_{HB}(t)$, obtained for the solutions studied. Panel (a) shows the curves corresponding to fructose−fructose (top), water−water (middle), and F−W hydrogen bonds (bottom). Panel (b) shows in detail the HB correlation functions for HBs between water molecules on a log−log scale.

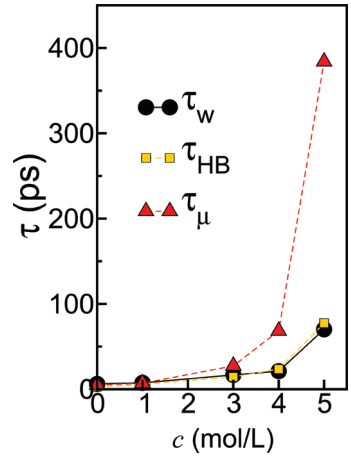

Figure 4. Water translational and orientational times (τ_w, with circles, and τ_μ, with triangles) and water−water H-bond relaxation times versus fructose concentration.

with the simulated curves. For completeness, the best fitting parameters and the corresponding HB relaxation times (τ_{HB}) are listed in Table 4. We observe that the stretched-exponential contributions account for less than one-third of the overall decays for the most dilute solution (1 M), while this proportion increases with concentration, reaching ~67% for $c = 5$ M. In contrast, the concentration dependence of the exponent β is very weak, i.e., $\beta \approx 0.35$, independent of the fructose content in the solution. As expected, the concentration dependence of the overall decay shows a progressive retardation of the HB breaking dynamics. The H-bond relaxation time for HBs between water molecules becomes longer with increasing sugar concentration (a factor of ~20 in passing from pure water to a 5 M solution). The concentration effects are more pronounced for fructose−water HBs, where the characteristic times may be stretched up to a factor of ~60 in passing from 1 to 5 M solutions.

In Figure 4 we display the characteristics of the water dynamics in different fructose solutions expressed in terms of the corresponding characteristic times for translational (τ_w), reorientational (τ_μ), and H-bond dynamics (τ_{HB}). All curves exhibit a gradual retardation at low and intermediate concentrations, say up to $c \sim 4$ M, followed by much sharper increments along the relatively narrow $4 \lesssim c \lesssim 5$ M interval. We also notice that the rise observed in τ_μ is much more pronounced than those exhibited by τ_w and τ_{HB}. This is likely to be due to the increasing fraction of water molecules involved in HBs with fructose: these waters would largely contribute to the slowdown of the orientational relaxation but not to the water−water HB dynamics considered.

In order to unveil a physical reason for such increments, we found it convenient to undertake a more detailed analysis of the statistics and topology of the overall intermolecular connectivity. In Figure 5 we display results for the average number of HBs in different solutions, n^{HB}. As expected, in passing from dilute to more concentrated solutions, the number of hydrogen bonds between water molecules decreases at the expense of an increasing number of sugar−water HBs. A similar analysis performed from the fructose perspective shows the reverse concentration trend. Namely, the number of F−F hydrogen bonds diminishes as we move to dilute solutions. Interestingly, there is practically a complete cancellation between these opposite effects, since the total number of HBs—regardless of the nature of the tagged partners—per water or fructose unit remains practically unchanged along the whole concentration range investigated ($n_w^{HB} \sim 3.5$ and $n_F^{HB} \sim 9.5$; see open circles and open triangle curves in Figure 5). The general picture that

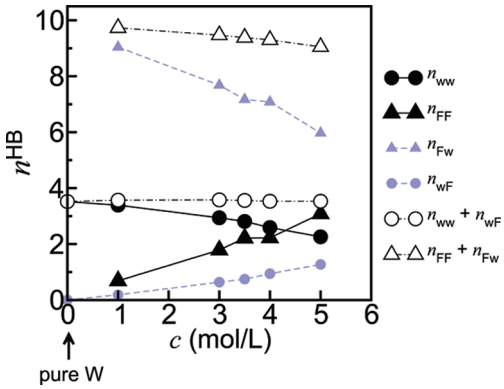

Figure 5. Average number of H bonds versus fructose concentration. n_{ab} represents the number of HBs between a and b species, per molecule of type a, where a, b = water (W), fructose (F). Open symbols correspond to the total average number of H-bonds per water (circles) and per fructose molecule (triangles).

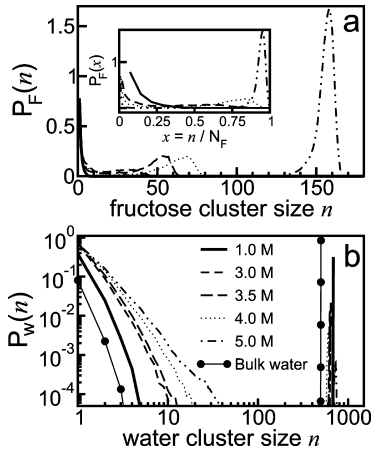

Figure 6. Probability of finding an arbitrary fructose [panel (a)] or water molecule [panel (b)] belonging to a cluster of size n at different compositions. The inset on panel (a) shows P_F as a function of the reduced variable x, where $x = n/N_F$ with N_F the total number of fructose molecules in the system.

emerges from these considerations is that in which water molecules can easily saturate all OH groups available for establishing HB connectivity, at a relatively reduced energy cost.

Based on the H-bonding geometrical criterion, we investigate the formation of molecular clusters, i.e., sequences of H-bonded molecules of species i (i = W, F). For a given configuration, once the overall connectivity pattern between different molecules is established, it is straightforward to generate distribution functions $P_i(n)$ representing the probability that a randomly chosen molecule of species i belongs to a cluster containing n molecules.

Cluster statistics results for fructose species are shown in Figure 6a. At low concentrations, the fructose molecules are found as isolated molecules or forming small disconnected clusters ($n \lesssim 10$), whereas in the midconcentration regime, $c \sim 3.5$ M, clusters of fructose as large as $n \sim 50$ are occasionally found. Sharp changes in $P_F(n)$ are found in the concentration range 4−5 M, where the shape of the distributions correspond to a single cluster containing a sizable fraction of the total number of molecules, complemented with a few additional monomers and dimers. From the water perspective, a similar connectivity analysis shows the complementary picture: while in pure water only 10% of the total population of molecules are found disconnected from the rest or forming dimers, at c = 5 M that percentage increases up to approximately 85% (see Figure 6b). In fact, simulation results of carbohydrate/water solutions reported by Roberts and Debenedetti[11] indicate the disappearance of full connectivity between water molecules at sugar concentrations intermediate between 60 and 80 wt %.

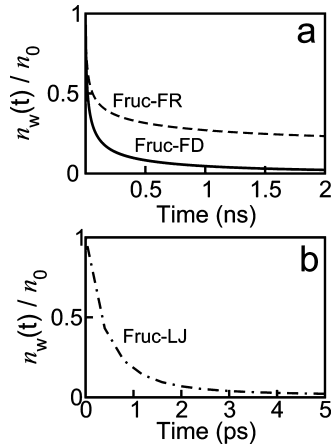

Figure 7. Survival probability function for hydration waters in a 5 M fructose solution, for the three types of dynamics considered. Note different time scales and units in panels (a) and (b).

C. Dynamics of Hydration Water. Without being rigorous in our description, we will refer to the above scenario as a structurally heterogeneous system, in which prevails a "percolative" fructose domain surrounded by "patchy" regions of water molecules. Moreover, this characterization leads to a natural partition of solvent molecules between those in intimate contact with the large cluster—hereafter referred as *bound* or *interfacial* water—and the rest, not directly connected with fructose units (*free* water). Given these characteristics, one can anticipate that the dynamics of bound water molecules will be very much hindered by two major reasons: (i) the slow dynamics governing the overall structural modifications in the "percolating" cluster and (ii) the topology and energetics (pinning) of the confinement prevailing at the boundaries between F and W domains that will restrict large amplitude modes.

To get quantitative estimates of these effects on the translational modes, we computed τ_r, average residence times, namely, the average time during which a given water molecule remains bound to the "percolating" cluster, for the 5 M system. Estimates for τ_r are obtained from TCFs[22,39,40]

$$n_w(t) = \sum_{j=1}^{N_w} \langle p_j(0) p_j(t) \rangle \qquad (7)$$

where the characteristic function $p_j(t)$ equals 1 if molecule j is adjacent to any of the fructose residues continuously along the time interval $[0, t]$ and zero otherwise.[22,24,41,42] A water molecule is considered to be adjacent to fructose if the interatomic distance between the water oxygen and any fructose atom is less than $r_c = (\sigma_w + \sigma_F)/2$, the arithmetic mean of the Lennard-Jones radii[43] of the aqueous oxygen and fructose atoms.

Results for $n_w(t)$ are displayed in Figure 7, and the best fitting parameters are listed in Table 5, where $n_0 \equiv n_w(t = 0) = 675$ corresponds to the equilibrium average number of hydration waters for the fully dynamical 5 M system. Practically 85% of the total number of water molecules can be considered as bound to the different sugar units, and the characteristic residence time is of the order of $\tau_r = 180$ ps.

Results for Fruc-FR and Fruc-LJ surrogate systems are also shown in Figure 7 and in the second and third rows of Table 5.

TABLE 5: Hydration Dynamical Parameters for 5 M Fructose Solutions. Part A: Stretched-Plus-Biexponential Fitting Parameters of the Survival Probability Function $n_w(t)/N_w$, Average Number of Hydration Waters (n_0), and Characteristic Residence Times (τ_r). Part B: Orientational Times (τ_μ) Obtained from Time Integrals of $C_1^\mu(t)$, for Bound and Free Waters. Part C: Translational Times (τ_w) and Power Law Parameter (α) Obtained from $\mathcal{R}_w^2(t)$ for Bound and Free Waters[a]

	A. hydration water survival probability[b]									B. orientational dynamics τ_μ		C. translational dynamics τ_w		C. translational dynamics α	
system	a_3	τ	β	a_1	τ_1	a_2	τ_2	n_0	τ_r	bound	free	bound	free	bound	free
Fruc-FD	0.68	16.3	0.55	0.12	247.8	0.08	1383	675	186.8	481.7	123.5	77.6	33.2	0.44	0.56
Fruc-FR[c]	0.53	20.2	0.51	0.11	476.9	0.24	10476	690	2970	13941	1845	685.2	144.8	0.32	0.46
Fruc-LJ[d]	0.00	–	–	0.13	0.74	0.011	3.83	207	1.65	9.81	9.05	10.6	10.6	0.51	0.60
bulk water										5.04		5.9		0.99	

[a] Times are given in picoseconds. [b] Fitting parameters correspond to fits of $n_w(t)/N_w$. [c] $C_1^\mu(t)$ fitted to an exponential function in the time range $1 \le t \le 10$ ns. [d] $n_w(t)$ fitted to a biexponential function, in the time range $1 \le t \le 100$ ps.

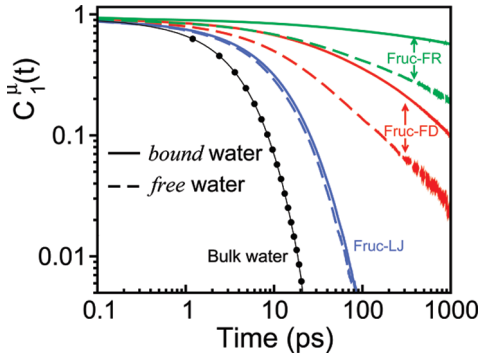

Figure 8. First-rank dipolar relaxation of waters in a 5 M fructose solution, for the simulated systems. Solid and dashed lines correspond to the TCFs of water molecules that are initially inside (*bound*) or outside (*free*) the fructose hydration shell, respectively. For comparison, the dipolar relaxation of bulk water is also displayed with circles.

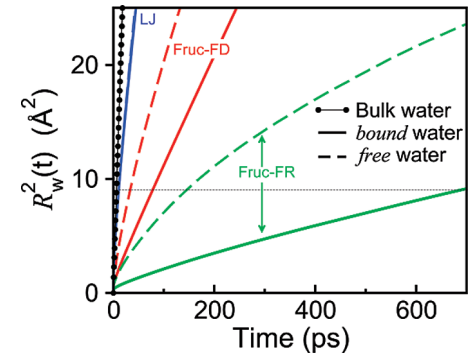

Figure 9. Mean-square displacement, $\mathcal{R}_w^2(t)$, of waters in a 5 M fructose solution, for the simulated systems. Solid and dashed lines correspond to the TCFs of water molecules that are initially inside (*bound*) or outside (*free*) the fructose hydration shell, respectively. For comparison, $\mathcal{R}_w^2(t)$ corresponding to bulk water is also displayed with circles. The dashed horizontal line corresponds to a water-squared diameter, $\mathcal{R}_w^2 = 9$ Å^2.

Note that the absence of solute dynamics does not modify substantially the number of interfacial water molecules, $n_0 = 690$, but it does stretch the characteristic residence time up to $\tau_r \sim 3$ ns. Even more prominent are the changes induced by the absence of F−W Coulomb coupling which leads to (i) structural modifications of the hydration shell characterized by a marked reduction in the population of the interfacial water down to $n_0 \sim 200$ and (ii) a much sharper reduction in the corresponding characteristic times, which have dropped down to the order of $\tau_r = 1.65$ ps. These behaviors are not unexpected, since in the absence of F−W electrostatic interactions, the fructose matrix behaves as a hydrophobic surface and promotes interfacial dewetting (water depletion).[44]

In order to provide further description of the dynamics at the hydration of layer, we analyzed its rotational and translational diffusive motions in comparison with the rest of the water molecules in the system. Figure 8 shows the first-rank dipolar relaxation for hydration (solid lines) and "bulk" waters (dashed lines), while the characteristic times obtained from the corresponding integrals are listed in Table 5. The combined effects of the (fully dynamical) confinement and the fructose−water Coulomb coupling lead to practically 2 orders of magnitude increase in the characteristic rotational time, $\tau_\mu = 480$ ps, for the hydration layer versus $\tau_\mu \sim 5$ ps for pure water. Note that the rotational hindrance is not at all negligible even for the *free* water, where the coupling with the nearby hydration waters and the not so distant fructose units takes τ_μ up to ∼120 ps.

Similarly to what was found for the residence times, the suppression of solute dynamics, as given by the Fruc-FR system, practically stretches the rotational relaxation of interfacial and free water beyond the nanosecond time scale, thus highlighting the importance of the full time-dependent structural fluctuations of the sugar clusters for the long-time components of the overall system dynamics. The effects are stronger for water molecules in the immediate vicinity of the solute. When the electrostatic interactions between water and fructose are suppressed (Fruc-LJ system), the rotational dynamics of surface and bulk waters become similar to each other ($\tau_\mu \sim 10$ ps) due to the lack of water−solute H-bonding, and much faster than in the presence of Coulombic coupling. Yet, in contrast to the rotational behavior found for water surrounding lysozyme, the dipolar relaxation of water molecules in the absence of the energetic disorder in concentrated fructose solution is nearly two times slower than in the neat liquid ($\tau_\mu \sim 5$ ps). This suggests, not unexpectedly, that the sugar aggregates constitute an environment that is substantially more spatially confining than the clefts of a globular protein. Moving away from a protein surface one encounters an open ocean of water which does not hamper the switching allegiance[33] that governs water reorientation, whereas in the concentrated saccharide solutions, water is predominantly found in spatially limited patchy regions where rotational dynamics becomes strongly hindered.

Results for the translational dynamics are shown in Figure 9, which depicts the mean-squared displacements (MSD) of water molecules in the hydration layer and away from the solute for the fully dynamic (FD), Fruc-FR, and Fruc-LJ systems. One notices that the translational motion for water molecules residing at the saccharide surface is slower, independent of the dynamics of the sugars, and that immobilizing the solute aggregate topology markedly suppresses water diffusion. The MSD at 5 M concentration can be well-fitted to a power law, $\mathcal{R}^2(t) = \langle|\mathbf{r}_i(t) - \mathbf{r}_i(0)|^2\rangle \propto t^\alpha$. The parameter α reported in the last column

of Table 5 indicates a sublinear regime ($\alpha < 1$) of translational diffusion for both bound and free water molecules. The exponent obtained for the MSD of the hydration waters corresponding to Fruc-FR is $\alpha = 0.32$, a smaller value than that found for Fruc-FD ($\alpha = 0.44$). This means that the sugar aggregate fluctuations—which are absent in Fruc-FR—reduce the anomalous character of hydration water translational diffusion, similarly to that reported for proteins.[25] The power law for Fruc-LJ yields $\alpha = 0.51$, a value a bit closer to the fully dynamic case, but yet much smaller than the bulk value ($\alpha \sim 1$).

To complete the comparison, we computed the characteristic time, τ_w, a diffusing water molecule takes to travel a distance equivalent to its own diameter (~3 Å) in each case (see Table 5). Relative to neat water, the characteristic translational time in the hydration layer increases more than an order of magnitude, from ~6 to ~78 ps, for the fully dynamical solute, and over 2 orders of magnitude in the absence of saccharide motions. Separating out the pinning effects of the Coulomb coupling from the surrogate system that contains both topological and energetic disorders (Fruc-FR), τ_w for Fruc-LJ drops down considerably to ~10 ps, not much bigger than the neat liquid value, despite the markedly non-Brownian character of its MSD time dependency (cf. α in Table 5).

The overall physical picture that emerges from these considerations suggests that in fructose solutions with concentrations of the order of $c \sim 4-5$ M the sharp increase in the different time scales describing the dynamical modes of water molecules could be ascribed to equally sharp modifications that take place in the microscopic connectivity of water and sugar domains. In this concentration regime, the vast majority of water molecules remain in close contact with sugar units, which, in turn, aggregate into mesoscopic clusters extending over tens of times the diameter of a water molecule. As such, and due to the strong Coulomb coupling that dominates solute−solvent interactions, the long-time dynamics of the water seems to be governed to a large extent by reactive mechanisms that control slow collective modes involving long wavelength changes in the cluster geometry. The separate effects from topological and energetic disorders on the translational and rotational diffusion of the hydration layer are similar to that recently reported for protein hydration.[25] However, the natures of the geometrical confinements at the surface of a globular protein and in concentrated carbohydrate solutions differ, leading to subtle, but potentially important, differences in the water dynamics in these systems. Whereas for protein hydration the rotational dynamics is altered by the energetic disorder alone, for concentrated fructose solutions the rotational relaxation is perturbed by both topological and energetic disorder.

IV. Concluding Remarks

The results presented in this paper provide information about the dynamical behavior of aqueous fructose solutions in a wide range of sugar concentrations. As expected, as the concentration of sugar is increased, a progressive slowdown effect is observed on the overall dynamics of the solvent and, even more markedly, on that of the solutes. Typical diffusive times of water in the most concentrated solution that we analyzed, $c \sim 5$ M, are 1 order of magnitude longer than in the pure aqueous phases, a variation which is in good agreement with direct experimental information. Slowdown effects are even more dramatically manifested in the lengthening of the characteristic times describing orientational motions of the solvent molecules, where the differences may involve up to a factor of ~80. Combined effects of these two motions get translated in equally important modifications in the H-bond relaxation times, most notably in those involving water−fructose bonds.

The concentration dependence of all dynamics shows sharp increments as one surpasses, say, $c \sim 4$ M. In this concentration regime, we also found important modifications operated in the overall structural arrangement of solute and water species. The changes can be pictured as a transition from a distribution of associated fructose molecules (with a number of units varying around 5−10 units) surrounded by a continuous aqueous environment to a scenario where a single mesoscopic cluster—encompassing a sizable fraction of the total number of solute molecules—prevails. Complementary to the solute structural changes, the structure of water can be portrayed as a collection of "patchy" domains adjacent to the boundary of the main sugar cluster and with a much restricted connectivity between them.

In order to establish a relationship between the observed features and those recently reported for protein solvation, we analyzed the effects arising from the suppression of the dynamical fluctuations of the "percolating cluster" and the subsequent switching off of the solute−solvent Coulomb coupling in order to investigate the separate effects arising from topological and energetic disorders on water dynamics. In agreement with results reported for the solvation of lysozyme, the absence of solute dynamics stretches all characteristic times in a sensible fashion, being always more prominent for those describing water rotational dynamics. On the other hand, the subsequent suppression of solute−solvent Coulomb coupling promotes the opposite effect and accelerates the dynamics, especially the rotational one, with a subtle distinction from the case of protein hydration in the sense that both energetic and topological disorders influence rotational dynamics in fructose solutions.

Acknowledgment. We are grateful to Professor Daniel Laria for several helpful discussions and valuable suggestions and for thoroughly reading this manuscript. M.H.H.P. acknowledges financial support from CONICET. M.D.E. is a staff member of CONICET (Argentina). M.S.S. thanks the Brazilian agencies FAPESP and CNPq for financial support.

References and Notes

(1) Tomasik, P. *Chemical and Functional Properties of Food Saccharides*; CRC Press: New York, 2003.
(2) Hill, S. E.; Ledward, D. A.; Mitchell, J. R. *Functional Properties of Food Macromolecules*, 2nd ed.; Springer: New York, 1998.
(3) Rampp, M.; Buttersack, C.; LüDeman, H.-D. *Carbohydr. Res.* **2000**, *328*, 561.
(4) Padua, G. W.; Schmidt, S. J. *J. Agric. Food. Chem.* **1992**, *40*, 1524.
(5) Mahawanich, T.; Schmidt, S. J. *Food Chem.* **2004**, *84*, 169.
(6) Baraguey, C.; Mertens, D.; Dölle, A. *J. Phys. Chem. B* **2002**, *106*, 6331.
(7) Fuchs, K.; Kaatze, U. *J. Phys. Chem. B* **2001**, *105*, 2036.
(8) Fuchs, K.; Kaatze, U. *J. Chem. Phys.* **2002**, *116*, 7137.
(9) Feeney, M.; Brown, C.; Tsai, A.; Neumann, D.; Debenedetti, P. G. *J. Phys. Chem. B* **2001**, *105*, 7799.
(10) Lelong, G.; Price, D. L.; Douy, A.; Kline, S.; Brady, J. W.; Saboungi, M.-L. *J. Chem. Phys.* **2005**, *122*, 164504.
(11) Roberts, C. J.; Debenedetti, P. G. *J. Phys. Chem. B* **1999**, *103*, 7308.
(12) Molinero, V.; Çağin, T.; Goddard, W. A., III. *Chem. Phys. Lett.* **2003**, *377*, 469.
(13) Molinero, V.; Çağin, T.; Goddard, W. A., III. *J. Phys. Chem. A* **2004**, *108*, 3699.
(14) Lee, S. L.; Debenedetti, P. G.; Errington, J. R. *J. Chem. Phys.* **2005**, *122*, 204511.
(15) Sonoda, M. T.; Skaf, M. S. *J. Phys. Chem. B* **2007**, *111*, 11948.
(16) Bhattacharyya, K.; Bagchi, B. *J. Phys. Chem. A* **2000**, *104*, 10603.
(17) Bagchi, B. *Chem. Rev.* **2005**, *105*, 3197.
(18) Pal, S. K.; Zhao, L. A.; Zewail, A. H. *Proc. Natl. Acad. Sci.* **2003**, *100*, 8113.

(19) Pal, S.; Maiti, P. K.; Bagchi, B.; Hynes, J. T. *J. Phys. Chem. B* **2006**, *110*, 26396.
(20) Andreatta, D.; Lustres, J. L. P.; Kovalenko, S. A.; Ernsting, N. P.; Murphy, C. J.; Coleman, R. S.; Berg, M. A. *J. Am. Chem. Soc.* **2005**, *127*, 7270.
(21) Bizzarri, A. R.; Cannistraro, S. *Phys. Rev. E* **1996**, *53*, R3040.
(22) Rocchi, C.; Bizzarri, A. R.; Cannistraro, S. *Phys. Rev. E* **1998**, *57*, 3315.
(23) Marchi, M.; Sterpone, F.; Ceccarelli, M. *J. Am. Chem. Soc.* **2002**, *124*, 6787.
(24) Bizzarri, A. R.; Cannistraro, S. *J. Phys. Chem. B* **2002**, *106*, 6617.
(25) Pizzitutti, F.; Marchi, M.; Sterpone, F.; Rossky, P. J. *J. Phys. Chem. B* **2007**, *111*, 7584.
(26) Damm, W.; Frontera, A.; Tirado-Rives, J.; Jorgensen, W. L. *J. Comput. Chem.* **1997**, *18*, 1955.
(27) Berendsen, H. J. C.; Grigera, J. R.; Straatsma, T. P. *J. Phys. Chem.* **1987**, *91*, 6269.
(28) Phillips, J. C.; Braun, R.; Wang, W.; Gumbart, J.; Tajkhorshid, E.; Villa, E.; Chipot, C.; Skeel, R. D.; Kale, L.; Schulten, K. *J. Comput. Chem.* **2005**, *26*, 1781.
(29) Martínez, J. M.; Martínez, L. *J. Comput. Chem.* **2003**, *24*, 819.
(30) Zhou, R.; Huang, X.; Margulis, C. J.; Berne, B. J. *Science* **2004**, *305*, 1605.
(31) Allen, M. P.; Tildesley, D. J. *Computer Simulation of Liquids*; Oxford University Press: New York, 1994.
(32) Luzar, A.; Chandler, D. *J. Chem. Phys.* **1993**, *98*, 8160.
(33) Luzar, A.; Chandler, D. *Nature* **1996**, *379*, 55.
(34) Laage, D.; Hynes, J. T. *Science* **2006**, *311*, 832.
(35) Laage, D.; Hynes, J. T. *J. Phys. Chem. B* **2008**, *112*, 14230.
(36) Rapaport, D. C. *Mol. Phys.* **1983**, *50*, 1151.
(37) Martí, J.; Padró, J. A.; Guàrdia, E. *J. Chem. Phys.* **1996**, *105*, 639.
(38) Borin, I. A.; Skaf, M. S. *J. Chem. Phys.* **1999**, *110*, 6412.
(39) Impey, R. W.; Madden, P. A.; McDonald, I. R. *J. Phys. Chem.* **1983**, *87*, 5071.
(40) Martins, L. R.; Ribeiro, M. C. C.; Skaf, M. S. *J. Phys. Chem. B* **2002**, *106*, 5492.
(41) Bizzarri, A. R.; Rocchi, C.; Cannistraro, S. *Chem. Phys. Lett.* **1996**, *263*, 559.
(42) Rocchi, C.; Bizzarri, A. R.; Cannistraro, S. *Chem. Phys.* **1997**, *214*, 261.
(43) The analytical expression employed for the Lennard-Jones contribution to the potential energy was $U_{LJ}(r) = 4\varepsilon[(\sigma/r)^{12}-(\sigma/r)^{6}]$.
(44) Giovambattista, N.; Debenedetti, P. G.; Rossky, P. J. *J. Phys. Chem. C* **2007**, *111*, 1323.

JP904019C